Taylor & Francis
Taylor & Francis Group

Fullerenes, Nanotubes and Carbon Nanostructures

ISSN: (Print) (Online) Journal homepage: www.tandfonline.com/journals/lfnn20

Is triple crossed C_{28} cyclic polyyne cluster a stable conformation?

Carmen E. Stoenoiu, Mihai V. Putz & Lorentz Jäntschi

To cite this article: Carmen E. Stoenoiu, Mihai V. Putz & Lorentz Jäntschi (2024) Is triple crossed C_{28} cyclic polyyne cluster a stable conformation?, Fullerenes, Nanotubes and Carbon Nanostructures, 32:1, 55-67, DOI: 10.1080/1536383X.2023.2261573

To link to this article: https://doi.org/10.1080/1536383X.2023.2261573

FULLERENES, NANOTUBES AND CARBON NANOSTRUCTURES
2024, VOL. 32, NO. 1, 55–67
https://doi.org/10.1080/1536383X.2023.2261573

Is triple crossed C_{28} cyclic polyyne cluster a stable conformation?

Carmen E. Stoenoiu[a,b], Mihai V. Putz[c,d], and Lorentz Jäntschi[e,f]

[a]Laboratory of Instrumental Analysis, Faculty of Automotive, Mechatronics and Mechanical Engineering, Technical University of Cluj-Napoca, Cluj, Romania; [b]Department of Department of Electric Machines and Drives, Faculty of Electrical Engineering, Technical University of Cluj-Napoca, Cluj, Romania; [c]Laboratory of Computational and Structural Physical-Chemistry for Nano-sciences and QSAR, Biology-Chemistry Department, Faculty of Chemistry, Biology, Geography, West University of Timişoara, Timişoara, Romania; [d]Scientific Laboratory of Renewable Energies-Photovoltaics, R&D National Institute for Electrochemistry and Condensed Matter (INCEMC-Timisoara), Timişoara, Romania; [e]Doctoral School of Chemistry, Faculty of Chemistry and Chemical Engineering, Babeş-Bolyai University, Cluj, Romania; [f]Department of Physics and Chemistry, Faculty of Engineering of Materials and Environment, Technical University of Cluj-Napoca, Cluj, Romania

ABSTRACT

Polyynes sometimes referred to as oligoynes or carbinoids, and their resonance cumulene form are valuable precursors to a whole series of more complex organic derivatives. Motivated by a series of studies that explore the stabilization of polyynes, in different ways, the possibility of their stabilization through the formation of crossed cycles is explored in this article. It is easy to notice that the cyclic conformations represent a special case, in that they possess an increased symmetry. The stability of the polyene molecule can be enhanced by building cross-clusters. In this article, the molecular modeling tools were employed in order to provide insights about the construction and stability of $3C_{28}$ triple crossed C_{28} cyclic polyyne cluster. It has been shown that C_{28} and $3C_{28}$ triple crossed C_{28} are very similar energetically. HOMO–LUMO gap suggests a metallic conductivity. The angles between the planes of the molecular rings shows almost an axial alignment of the rings. A symmetry-constrained optimization was conducted using Z-matrix internal coordinates and Gaussian software, and it revealed that the geometrical conformation of C_{28} polyyne as triple crossed cluster is a stable conformation, since in all investigated scenarios the convergence is assured and it is to nearly optimum local points.

ARTICLE HISTORY
Received 6 August 2023
Accepted 15 September 2023

KEYWORDS
Polyynes; molecular clusters; density functional theory (DFT)

1. Introduction

Even if polyynes have been isolated from a wide variety of cultures of higher fungi,[1] different plant species,[2–6] bacteria,[7] marine sponges,[8,9] and even corals,[10] and they represent a unique class of compounds with antibacterial,[11] anticancer,[12] antimicrobial,[13] antifeedant[14] antifungal,[15] anti-HIV,[16,17] antitumor,[18] and pesticidal[19] activies, their full potential in the pharmaceutical and medical fields has not yet been exhaustively explored (for instance, as vitamins carriers[20]). The conjugation of the triple bonds appears to be a very effective inhibitor of transient receptor potential channels of ankyrin type-1 for some endemic plants,[21] but recent discoveries of the role of some polyynes produced by bacteria as chemical weapons against hosts and competitors[22] put the research of polyynes into a new light for medical use.

All biologically produced polyynes and most of the synthetic ones are small, because the stability of the linear polyynes decreases with their length.

The recent rediscovery of polyyne molecules[23] (carbine in Ref. [24]) is due to their unique features of single and triple bond alternation. Oligomeric cousins of carbine are of scientific interest as well, as linear or cyclic complexes.[25] If a single C–C bond has an average distance of 1.53–1.54 Å and dissociation energy of 3.6–3.9 eV, then the presence of a double or triple bond updates these values to about 1.33 Å and 7.4 eV and to about 1.20 Å and 10 eV, respectively.[26] With an average of 22% in length compared to a single bond and of 13% compared to an aromatic bond, and a 167% average increase in energy compared to a single bond and of 83% compared to aromatic bond, the triple bonds between Carbon atoms are very attractive for applications requiring dense materials[27] with very good compressibility.[28] The space inside polyyne, carbene, carbine, and other planar and approximately planar rings may facilitate formation of complexes.[29] A series of more polar compounds results when Boron and Nitrogen replaces Carbon in a regular manner.[30,31]

The resonance between open-shell biradical structure (polyyne form) and closed-shell Kekulé structure (cumulene form) is the key to getting an entire series of derivatives.[32,33] Its immediate use is to arrive to poly-functionalized compounds[34] and π-conjugated polymers,[35,36] but,

CONTACT Mihai V. Putz mihai.putz@e-uvt.ro Laboratory of Computational and Structural Physical-Chemistry for Nano-sciences and QSAR, Biology-Chemistry Department, Faculty of Chemistry, Biology, Geography, West University of Timişoara, Timişoara, Romania; Lorentz Jäntschi lorentz.jantschi@gmail.com Department of Physics and Chemistry, Faculty of Engineering of Materials and Environment, Technical University of Cluj-Napoca, Cluj, Romania

nevertheless, polyyne form $((-C\equiv)_n)$ structure is favored[37] over cumulene $((=C=)_n)$.

Experimental,[38–40] theoretical,[37,41–43] and review[44–46] studies were dedicated to characterize polyyne.

While synthesizing an abundance of small and medium-sized chains ($n \leq 32$) was reported some time ago,[47] very good yields (72%, 36%, and 51% for $n = 20$, 24, and 28, respectively) were more recently reported.[48] A long chain ($n > 300$) was reportedly being synthesized as well.[49] Separation techniques made progress as well.

The tendency of the polyynes to form rings was observed (when $22 \leq n \leq 46$) at laser vaporization of graphite as a secondary product in the synthesis of fullerenes in Ref. [50]. Meanwhile, the separation techniques have progressed.[51] Since cumulenes may act as reactive intermediates,[52] synthetic routes to cyclic compounds may simply require a conformational lock.[53]

Cyclization of polyynes ($n = 10, 14$ and 18 in Ref. [54]; 24 in Ref. [55]; $n = 18, 22, 26$ and 30 in Ref. [56]) may provide further insight into their stabilization, and the same applies for cumulenes.[57,58] Moreover, old[59,60] and new[46,55] studies are in support of the fact that certain rings are more stable than linear chains. Specifically, in Ref. [55] it is noted that rings are more likely to appear when $n \geq 14$ and $n = 4 \cdot k$ ($n = 16, 20, 24, 28, \ldots$).

Pieces of evidence that crosslinking of the chains stabilizes molecules as a cluster are Refs. [61,62] and [63].

The stability of the unsaturated polyynic/cumulenic configuration can be further increased by condensation. In this article, results about the stability of C_{28} are communicated, as well as the potential of further increase for its stability by condensing as a triple crossed cluster.

2. Methods

For selecting the appropriate method of further optimization, a comparison study was conducted on a much simpler molecule (N≡N, see Table 1).

The study was conducted in a much deeper extent (among others also Møller Plesset's MP2) but Table 1 contains, for simplification, only the methods significant in connection with the results (BP) along with three others. As Table 1 reveals (see entry BP/6-311G* in Table 1; $\Delta_r = \frac{191.61-191.61}{191.61} + \frac{20.81-20.80}{20.81} + \frac{14.01-13.94}{14.01} + \frac{110.8-109.8}{109.8} = 1.5\%$), the lowest departure between the model and experiment for the selected set of properties appears first at DFT BP 6-311G* (theory level, exchange and correlation functional, basis set), which was selected as the final working package of the optimization for the cluster.

Table 1. Experimental vs. calculated (at two theory levels) values for Four properties at N≡N.

Basis set	M1	M2	M3	M4	Δ_r
Experimental data					
	191.61	20.81	13.94	109.8	0.0
Method: HF					
STO-3G	191.99	20.79	15.97	113.4	18.1
3-21G	191.23	20.79	15.62	108.3	13.7
6-31G*	191.16	20.79	16.49	107.8	20.4
6-31G**	191.16	20.79	16.49	107.8	20.4
6-31 + G*	191.16	20.79	16.46	107.8	20.2
6-311G*	191.03	20.79	16.39	107.0	20.5
6-311 + G**	191.04	20.79	16.35	107.1	20.1
Method: BP					
6-31G*	191.75	20.8	14.05	111.8	2.7
6-31G**	191.75	20.8	14.05	111.8	2.7
6-31 + G*	191.74	20.8	14.05	111.7	2.6
6-311G*	191.61	20.8	14.01	110.8	1.5
6-311 + G**	191.61	20.8	14.01	110.8	1.5
6-311++G**	191.61	20.8	14.01	110.8	1.5
Method: BLYP					
6-31G*	191.95	24.96	13.35	111.8	26.2
6-31G**	191.95	24.96	13.35	111.8	26.2
6-31 + G*	191.95	24.96	13.31	111.8	26.5
6-311G*	191.95	24.97	12.81	110.8	29.2
6-311 + G**	191.95	24.97	12.81	110.8	29.2
6-311++G**	191.95	24.97	12.81	110.8	29.2
Method: B3LYP					
6-31G*	191.95	24.96	13.42	110.6	24.6
6-31G**	191.95	24.96	13.42	110.6	24.6
6-31 + G*	191.95	24.96	13.38	110.5	24.8
6-311G*	191.95	24.97	12.90	109.5	27.9
6-311 + G**	191.95	24.97	12.89	109.6	27.9
6-311++G**	191.95	24.97	12.89	109.6	27.9

Note: All data is given at normal ($T = 298.15$ K and $p = 101{,}325$ N · m^{-2}) temperature (T) and pressure (p). M1 = S^o (J · mol^{-1} · K^{-1}); M2 = C_v (J · mol^{-1} · K^{-1}); M3 = *ZPE* (kJ · mol^{-1}); M4 = $d_{N,N}$ (pm); $\boldsymbol{\Delta_r} = \sum_{i=1}^{4} \Delta_{r,i}$, in %. $\Delta_{r,i} = \frac{|Value_{Experimental,Mi} - Value_{Method,Mi}|}{Value_{Experimental,Mi}}$, $i = 1, 2, 3, 4$.

HF: Restricted Hartree-Fock [64–67]; BP: Density Functional Theory (DFT, [68,69]) BP86 (with Exchange = Becke [70], Correlation = Perdew [71]); BLYP: DFT BLYP (with Exchange = Becke [70], Correlation = LYP [72]); DFT B3LYP (with Exchange = 0.2 Hartree-Fock + 0.08 Slater + 0.72 Becke [73], Correlation = 0.81 LYP + 0.19 VWN1RPA [73,74]). Ref. for experimental data: [75]. Spartan'14 software was used [76] for calculations.

2.1. Cluster topology analysis

Cluster topology can be characterized by the crosses between the rings. In a way, crossing two rings in a cluster is similar to connecting two atoms with a bond in a molecule: once crossed (respectively connected), the reverse can be obtained only if the bond is disconnected. Considering cluster topology is specified by the crosses between rings, it is a distinct possibility to keep two rings together by crossing-over the rings, which is similar to connecting two atoms by a bond (see Figure 1). But the bunch of van der Waals effects acting in the interlocked rings follow a different physics than the nominal bond, so one can see the similarity more like a convention for the sake of topological language.

If a molecular topology ([77]; table 2 in Ref. [78]) is defined by a series of bonds (general case in Equation (1) with v_i atoms and e_j bond orders) which is $1, 2, 1$ for the diatomic molecule depicted in Figure 1 then a cluster topology ([79]; figure 10 in Ref. [43]) is defined by a series of crosses (general case in the same Equation (1), only with the meanings changed: v_i molecules and e_j number of in-between crosses).

$$v_1, v_2, e_1 \quad \ldots \tag{1}$$

2.2. Cluster geometry analysis

Each polyyne is the cyclic version of the linear one (see Figures 2 and 3) having the capping hydrogens removed.

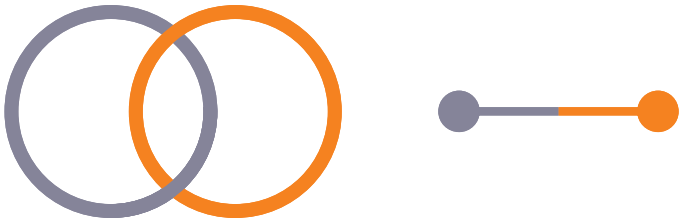

Figure 1. Crossing of two molecular rings (left) and the chemical bond (right).

Figure 2. Hydrogen capped $C_{28}H_6$ (linear) polyyne.

Figure 3. Hydrogen capped $C_{28}H_2$ (linear) polyyne.

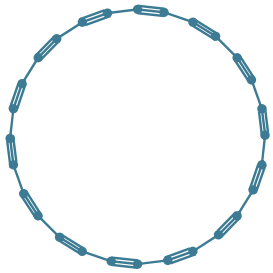

Figure 4. Cyclic C_{28} polyyne.

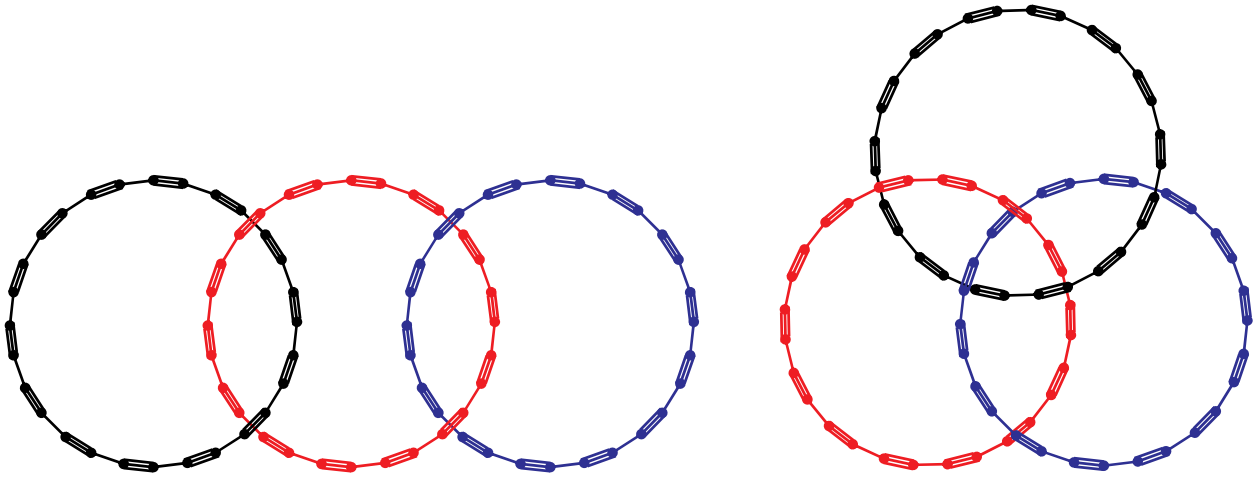

Figure 5. Cluster topology for two (left) and three (right) crosses of three cyclic polyynes.

Bending the polyyne is expected to be costly regarding the stability, but the formation of another bond is expected to at least partly compensate. For this reason, the energies were calculated and given for comparison (see § 3).

A separate study was employed, in which the stable geometric conformation of C_{28} polyyne (in Figure 4) was optimized.

Optimizing the geometry of a cluster is much more complex than that of a simple ring. After topology was defined (see § 2.1), the initial cluster geometry was optimized using the software reported in §3 of Ref. [43]. In this stage, the atoms were frozen inside of the molecule, and for each molecule, 7 degrees of freedom (3 for the center of the molecule, 3 for defining the plane of the molecule, and 1 for rotation for the molecule around its symmetry axis) were subject of finding; minimizing the sum of the inverses of the fourth power of the distances between atoms was found to be suitable for solving the problem (for more details please see[43]).

Next, the geometry optimization (energy minimization) was applied (until convergence) for DFT BP 6-311G* (178 + 38 optimization steps).

In the case of the cyclic C_{28} polyyne (see Figure 4), the analysis using DFT BP 6-311G* model has revealed that the bonds are approximately equal (C–C (single) bonds: 1.3256 Å with a standard deviation of $4 \cdot 10^{-5}$ Å; C≡C (triple) bond: 1.2534 Å with a standard deviation of $8 \cdot 10^{-6}$ Å). The fluctuation inside each type is very small, so with a

Table 2. DFT BP 6-311G* minimized energy data.

Object	Value	Remark
Total energy (in Hartree):		
H_2	−1.17505	DFT BP 6-311 G* value
$C_{28}H_6$	−1070.17173	Represented in Figure 2
$C_{28}H_2$	−1067.68073	Represented in Figure 3
C_{28}	−1066.45763	Represented in Figure 4
$3C_{28}$ (3×)	−3199.36045	Represented 2D in Figure 5 bottom
C −C bond length (in Å):		
$C_{28}H_6$	1.341	Bonds: 2×1.31, 6×1.32, 2×1.33, 2×1.34, 2×1.45
$C_{28}H_2$	1.321	Bonds: 5×1.31, 6×1.32, 2×1.33, 2×1.34, 0×1.45
C_{28}	1.3256	Standard deviation: $4 \cdot 10^{-5}$ Å
$3C_{28}$ (3×)	1.3257	Standard deviation: $1 \cdot 10^{-4}$ Å
$C \equiv C$ bond length (in Å):		
$C_{28}H_6$	1.2523	Bonds: 2×1.23, 0×1.24, 4×1.25, 7×1.26
$C_{28}H_2$	1.2514	Bonds: 2×1.23, 2×1.24, 2×1.25, 8×1.26
C_{28}	1.2534	Standard deviation: $8 \cdot 10^{-6}$ Å
$3\,C_{28}$ (3×)	1.2535	Standard deviation: $8 \cdot 10^{-5}$ Å
Highest occupied molecular orbital energy (HOMO, in eV):		
$C_{28}H_6$	−5.40	LUMO energy: −4.26 eV
$C_{28}H_2$	−5.65	LUMO energy: −4.56 eV
C_{28}	−5.55	LUMO energy: −4.93 eV
$3\ C_{28}$ (3×)	−5.52	LUMO energy: −4.92 eV

certain confidence it can be said that the bonds of each type are of the same length.

3. Results and discussion

3.1. General data for $3C_{28}$ triple crossed C_{28} cyclic polyyne cluster

Figure 5 gives (the) two different topologies of crossing three cyclic polyynes: with two and with three crosses.

In terms of topology (see Equation (1)), the double crossed $3C_{28}$ polyyne (Figure 5 left) is defined by $\{(1,2,1), (2,3,1)\}$, and corresponds to the molecular topology of propene ($<$), while the triple crossed $3\,C_{28}$ polyyne (Figure 5 right) is defined by $\{(1,2,1),\ (1,3,1),\ (2,3,1)\}$, and corresponds to the molecular topology of cyclopropene ($\mathcal{C}$).

The total energy data obtained from DFT BP 6-311G* (see Table 2) shows a loss of about 0.19 Hartree to bend $C_{28}H_6$ and form from it the C_{28} polyyne ($E(C_{28}H_6) - E(C_{28}) - 3E(H_2) = 0.19$ Hartree), and even less than that, 0.05 Hartree, when starting from $C_{28}H_2$ ($E(C_{28}H_2) - E(C_{28}) - E(H_2) = 0.05$ Hartree). The values above ($3 \cdot 0.05$ Hartree < 0.19 Hartree) are in line with expectations; the polyynic system (like the cumulenic one) is highly unsaturated (in deficit of electrons, which can be partly gained from Hydrogen atoms), and the addition of a larger number of hydrogen atoms brings the system closer to its most energetically favorable state. On the other hand, the same values suggest that $C_{28}H_2$ is in a closer energy state to the cyclic polyyne, and therefore is more likely to bend and cyclize.

When expressed per proton (or per electron), the total energy of the triple-crossed $3C_{28}$ cyclic polyyne is greater than the one of C_{28} with about 10^{-5} Hartree, which indicates a good potential to get a condensed state of C_{28} as triple crossed $3C_{28}$. The difference is slightly higher than the one for $3C_{26}(3\times)$. Bond lengths reveal that the increase in length of the double bond by condensation of the C_{26} into the triple crossed $3C_{28}$ cluster is insignificant (0.001 Å for both single and triple bons), but it exists; it may be caused by a slightly sterical constraint in the cluster. Two comments are to be made here. First, in some instances it is beneficial to be slightly constrained, such as when changing the allotropic state is intended; one should remember that artificial diamonds are obtainable from high pressure shocks on graphite grains. Second, if $3\,C_{28}(3\times)$ cluster is slightly constrained, then perhaps its next congener, $3C_{30}(3\times)$ better accommodates clusters of Carbon atoms. The HOMO–LUMO gap is systematicaly decreased (see Table 3) from 1.14 eV (at $C_{28}H_6$) to 1.09 eV (at $C_{28}H_2$), to 0.62 eV (to C_{28}), and to 0.60 eV (to $3C_{28}(3\times)$). Noticing that compounds with less than 0.5 eV reveal metallic conductivity in the solid state [80] makes $3C_{28}(3\times)$ a desirable target for electronics applications.

3.2. Further characterization of $3C_{28}$ triple crossed C_{28} cyclic polyyne cluster

The geometry of $3C_{28}$ triple crossed C_{28} polyyne cluster ($3C_{28}(3\times)$) has been subjected to geometry optimization using DFT BP 6-311G*. A large amount of time is required for the calculation. The optimized geometry is depicted in Figure 6 and the electronic density is depicted in Figure 7, while the Cartesian geometric coordinates of the atoms are given in the Appendix A.3.

Since all the above are purely informative and did not provide a characterization, a further investigation has been conducted.

The $3C_{28}(3\times)$ cluster possesses both RAMAN and IR active vibrations. A relatively large number of vibrations can be listed ($3 \cdot 3 \cdot 28 - 6$ are expected), however, of interest are the most intense ones (see Figure 8).

Please note that the vibration analysis should be conducted on the same level of theory and with the same basis set as the geometry optimization, otherwise, the obtained frequencies have no meaning since the first derivatives of the energy with respect to displacement of the atoms are zero only in that instance.

Table 3. Cluster conformation from DFT BP 6-311G* minimized energy data.

Parameter	Value
Center coordinates ((x,y,z), in Å, ± standard deviation):	
mol 1	$(+3.846_{\pm 0.006}, -0.115_{\pm 0.006}, -0.040_{\pm 0.006})$
mol 2	$(-0.024_{\pm 0.035}, +0.220_{\pm 0.035}, +0.069_{\pm 0.035})$
mol 3	$(-3.824_{\pm 0.035}, -0.121_{\pm 0.006}, -0.025_{\pm 0.035})$
Molecular torus radius (in Å, ± standard deviation):	
mol 1	$5.759_{\pm 0.011}$
mol 2	$5.758_{\pm 0.061}$
mol 3	$5.759_{\pm 0.011}$
Versors ((v_x, v_y, v_z), in Å, ± standard deviation):	
mol 1	$(-0.029_{\pm 0.024}, -0.873_{\pm 0.011}, -0.487_{\pm 0.018})$
mol 2	$(+0.039_{\pm 0.023}, -0.999_{\pm 0.022}, +0.023_{\pm 0.001})$
mol 3	$(+0.031_{\pm 0.020}, -0.874_{\pm 0.009}, +0.484_{\pm 0.016})$
Rotation angle on Oz, in °, to get first atom on Ox:	
mol 1	2.40
mol 2	−13.48
mol 3	1.76
In between angles, in °, ± standard deviation):	
mol 1 vs. mol 2	$60.5_{\pm 0.06}$
mol 1 vs. mol 3	$58.2_{\pm 0.05}$
mol 2 vs. mol 3	$61.7_{\pm 0.05}$

Note: All atoms have the coordinates given in Appendix 4: mol 1 is defined by the first 28 lines; mol 2 is defined by lines 29–56; mol 3 is defined by lines 57–84.

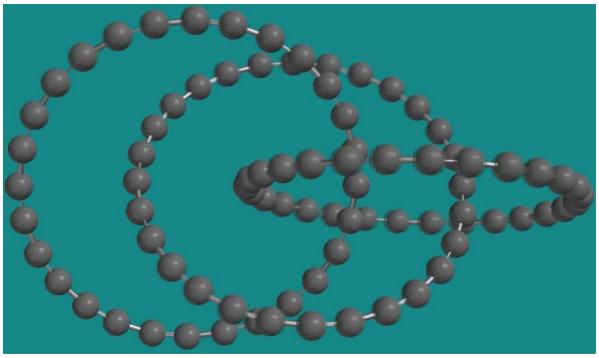

Figure 6. 3D perspective of $3C_{28}(3\times)$ cluster.

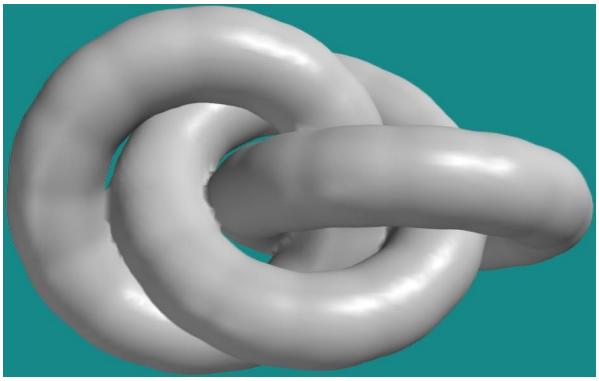

Figure 7. Electronic density at $3C_{28}(3\times)$ cluster at 0.001 e $^0/Å^3$.

Since the cluster is big and the molecules are disconnected, it is expected to be difficult to reach a minimum stationary point so the computation of the vibrations produces some imaginary frequencies. It is known that accuracy of the computation may produce false positive imaginary frequencies, so calculations were run with very high accuracy (`SCFTolerance = VeryHigh` in Spartan, equivalent of `Opt = VeryTight` in Gaussian). However, for a very small basis set (STO-3G), optimization followed by vibration analysis of $3C_{28}(3\times)$ produced 0 imaginary frequencies and a total of 241 distinct ones. Moving on to the next basis set (3-21G), there appeared 1 imaginary frequency and a total of 242 distinct ones, and in the next (6-31G) , there appeared 2 imaginary frequencies and a total of 243 distinct ones (from 246 expected). Other authors have observed similar behaviors.[81,82] One may argue it is expected that, using bigger and bigger basis sets, at a certain point all expected frequencies appear, but, according to the trend, all surplus ones are expected to appear imaginary. Going further, this suggests that $3C_{28}(3\times)$ cluster is energetically in a saddle point and easily may break apart or, more likely, convert into a more stable configuration. Note that there are 24 isomers for C_{84} fullerene[83] in which $3C_{28}(3\times)$ may convert. There are several ways that can explore the stability of the cluster in more detail, including further *ab initio* calculations[84] and the calculation of phonon dispersion.[85,86]

Calculating coordinates of the centers of the rings and of the versors perpendicular to their planes allows the evaluation of the radii of the rings, as well as of the angles between them (see Table 3).

The relative position of the rings and their orientation, along with the topology of the cluster are probably the key topological and geometrical invariants. Formally, the cluster topology is defined by molecules' composition in atoms as well as by the crosses between the rods (Equation (2)):

$$\begin{aligned} &\text{mol } 1: \ \text{atom}_1, \ldots, \text{atom}_{28} \\ &\text{mol } 2: \ \text{atom}_{29}, \ldots, \text{atom}_{56} \\ &\text{mol } 3: \ \text{atom}_{57}, \ldots, \text{atom}_{78} \\ &\text{cross } 1: \ \text{mol } 1, \text{mol } 2 \\ &\text{cross } 2: \ \text{mol } 1, \text{mol } 3 \\ &\text{cross } 3: \ \text{mol } 2, \text{mol } 3 \end{aligned} \tag{2}$$

It should be noticed that the values of the angles between the molecular rings of the cluster (see Table 3) are close to the values of a perfect split of a full rotation (60°) while, again, the topology of the cluster corresponds to the molecular topology of cyclopropene ($\mathcal{C}$).

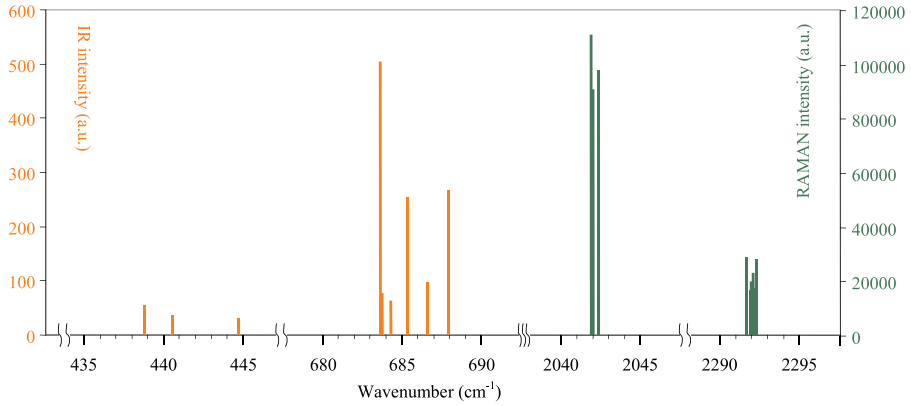

Figure 8. RAMAN and IR vibrations having at least 5% relative Intensity (from the most intense line).

Table 4. Z-matrix specification of symmetry constrained C_{28} cyclic polyyne.

Topology						
C						
C	1	c_0				
C	2	c_1	1	c_2		
…						
C	$2k+1$	c_0	$2k$	c_2	$2k-1$	c_3
C	$2k+2$	c_1	$2k+1$	c_2	$2k$	c_3
…						
C	1	c_1	2	c_2	3	c_3

Note: c_0, c_1, c_2, and c_3 are numeric floating point values and $k = 1, 2, \ldots, 12$.

3.3. The symmetrical alignment of atoms and molecules

Revealed in Figure 6, but more evident in Figure 7, is that the arrangement of the molecules is with the coordinates of the approximately axial centers and their molecular planes twisted. The analysis presented in Table 3 shows that these angles are approximately 60 degrees (60.5, 58.2, and 61.7 in Table 3).

One can therefore see the natural situation in which each molecule is considered approximately flat, in which case the number of degrees of freedom is dramatically reduced (from $3 \times 28 - 28$ to $3 + 3 + 1$). Once this assumption is accepted, that the molecule can be planar, the geometric optimization should follow this constraint. It is possible to make a new optimization of the molecular geometry, taking into account this constraint. In this case, the molecular topology must be specified so as to take into account the constraint. One possibility is using the Z-matrix syntax, which is an elegant way to represent the molecule in a delocalized internal coordinate system.[87]

It is relatively simple to specify a single molecule that is subject to constraints due to chemical bonds. Thus, the C_{28} cyclic polyyne can be specified as in Table 4.

The closest symmetrical conformation to the asymmetrical one is the one in which $c_0 = 1.3257$ Å, $c_1 = 1.2535$ Å, $c_2 = 167.10^{\circ}$, and $c_3 = 0.06^{\circ}$, but this is not optimal.

In the Table 4 topology, the condition for the molecule to be planar is $c_3 = 0^{\circ}$, so for an optimization in which the planarity of the molecule is a constraint, $c_3 = 0^{\circ}$ is a constant.

The Table 4 topology can be used to obtain the symmetrical molecular conformation relatively quickly. Starting from the values $c_0 = 1.3257$ Å, $c_1 = 1.2535$ Å, and $c_2 = 167.10^{\circ}$, with $c_3 = 0.0^{\circ}$ set as constant, BP 3-21 G identifies as the minimum energy conformation the one in which $c_0 = 1.3257$ Å, $c_1 = 1.2548$ Å, and $c_2 = 167.14^{\circ}$ (after 105 steps with Gaussian 09w[88]).

Specifying the C_{28} cyclic polyyne in internal coordinates by using the Z-matrix file provided a natural way to express and constrain the symmetry of the molecule. Upon taking a closer look to the Z-matrix in Table 4, only four variables are there (c_0 to c_3, two distances – c_0 and c_1 – and two angles – c_2 and c_3) instead of 3×28 if one refers to the Cartesian, or $3 \times 28 - 28$ considering the constrains given by the bonds.

To specify the positioning of the second molecule in relation to the first and respectively of the third in relation to the second (Table 5) is slightly more difficult.

As in the case of cyclic C_{28} polyyne, in the case of $3C_{28}$ there are two constraints that can be set constant: $a_0 = 167.14^{\circ}$ and $d_0 = 0.0$.

The $3C_{28}(3\times)$ cluster can be subjected to constrained optimization with the above given topology. Gaussian 09w[88] was used staring from various initial values and the results are given in Tables 6 and 7.

In the previous list r_1, r_2, b_1 and b_3 are distances (in Å), a_1, a_2, a_3 and a_4 are bond angles (in °, between 0° and 180°) and d_1, d_2, d_3, d_4, d_5 and d_6 are dihedral angles (in °, between 0° and 360°). All the optimizations listed in Tables 6 and 7 were convergent (see as proof HF 3-21 G and BP 3-21G Gaussian outputs in Appendix A.4) and support the hypothesis of the of the stability of the $3C_{28}(3\times)$ polyynic system. Optimum values proposed by the different optimization methods (see *Optimized values* columns in Tables 6 and 7) are very close to each other, suggesting that the difference is only due to method and basis set refinement levels.

An even greater benefit is the use of the symmetry constrains expressed in the terms of the Z-matrix to optimize the geometry of the cluster (Table 5) than it was for optimizing the geometry of the molecule (Table 4). Please note also that the use of the symmetry dramatically reduces the complexity of the cluster optimization problem, to 16 variables instead of $3 \times 3 \times 28$ (without bond constrains) or $3 \times (3 \times 28 - 28)$ with bond constrains.

It must be recognized that, for most applications, the levels of theory used here (HF and BP) are considered crude,

Table 5. Z-matrix specification of symmetry constrained $3\,C_{28}(3\times)$ cyclic polyyne cluster.

						Topology
C1						
C2	1	b_1				
C3	2	b_3	1	a_0		
C4	3	b_1	2	a_0	1	d_0
C5	4	b_3	3	a_0	2	d_0
C6	5	b_1	4	a_0	3	d_0
C7	6	b_3	5	a_0	4	d_0
C8	7	b_1	6	a_0	5	d_0
C9	8	b_3	7	a_0	6	d_0
C10	9	b_1	8	a_0	7	d_0
C11	10	b_3	9	a_0	8	d_0
C12	11	b_1	10	a_0	9	d_0
C13	12	b_3	11	a_0	10	d_0
C14	13	b_1	12	a_0	11	d_0
C15	14	b_3	13	a_0	12	d_0
C16	15	b_1	14	a_0	13	d_0
C17	16	b_3	15	a_0	14	d_0
C18	17	b_1	16	a_0	15	d_0
C19	18	b_3	17	a_0	16	d_0
C20	19	b_1	18	a_0	17	d_0
C21	20	b_3	19	a_0	18	d_0
C22	21	b_1	20	a_0	19	d_0
C23	22	b_3	21	a_0	20	d_0
C24	23	b_1	22	a_0	21	d_0
C25	24	b_3	23	a_0	22	d_0
C26	25	b_1	24	a_0	23	d_0
C27	26	b_3	25	a_0	24	d_0
C28	27	b_1	26	a_0	25	d_0
C29	28	r_1	27	a_1	26	d_1
C30	29	b_1	28	a_2	27	d_2
C31	30	b_3	29	a_0	28	d_5
C32	31	b_1	30	a_0	29	d_0
C33	32	b_3	31	a_0	30	d_0
C34	33	b_1	32	a_0	31	d_0
C35	34	b_3	33	a_0	32	d_0
C36	35	b_1	34	a_0	33	d_0
C37	36	b_3	35	a_0	34	d_0
C38	37	b_1	36	a_0	35	d_0
C39	38	b_3	37	a_0	36	d_0
C40	39	b_1	38	a_0	37	d_0
C41	40	b_3	39	a_0	38	d_0
C42	41	b_1	40	a_0	39	d_0
C43	42	b_3	41	a_0	40	d_0
C44	43	b_1	42	a_0	41	d_0
C45	44	b_3	43	a_0	42	d_0
C46	45	b_1	44	a_0	43	d_0
C47	46	b_3	45	a_0	44	d_0
C48	47	b_1	46	a_0	45	d_0
C49	48	b_3	47	a_0	46	d_0
C50	49	b_1	48	a_0	47	d_0
C51	50	b_3	49	a_0	48	d_0
C52	51	b_1	50	a_0	49	d_0
C53	52	b_3	51	a_0	50	d_0
C54	53	b_1	52	a_0	51	d_0
C55	54	b_3	53	a_0	52	d_0
C56	55	b_1	54	a_0	53	d_0
C57	56	r_2	55	a_3	54	d_3
C58	57	b_1	56	a_4	55	d_4
C59	58	b_3	57	a_0	29	d_6
C60	59	b_1	58	a_0	57	d_0
C61	60	b_3	59	a_0	58	d_0
C62	61	b_1	60	a_0	59	d_0
C63	62	b_3	61	a_0	60	d_0
C64	63	b_1	62	a_0	61	d_0
C65	64	b_3	63	a_0	62	d_0
C66	65	b_1	64	a_0	63	d_0
C67	66	b_3	65	a_0	64	d_0
C68	67	b_1	66	a_0	65	d_0
C69	68	b_3	67	a_0	66	d_0
C70	69	b_1	68	a_0	67	d_0
C71	70	b_3	69	a_0	68	d_0
C72	71	b_1	70	a_0	69	d_0
C73	72	b_3	71	a_0	70	d_0
C74	73	b_1	72	a_0	71	d_0
C75	74	b_3	73	a_0	72	d_0
C76	75	b_1	74	a_0	73	d_0
C77	76	b_3	75	a_0	74	d_0
C78	77	b_1	76	a_0	75	d_0
C79	78	b_3	77	a_0	76	d_0
C80	79	b_1	78	a_0	77	d_0
C81	80	b_3	79	a_0	78	d_0
C82	81	b_1	80	a_0	79	d_0
C83	82	b_3	81	a_0	80	d_0
C84	83	b_1	82	a_0	81	d_0

Note: a_0, a_1, a_2, a_3, a_4, d_0, d_1, d_2, d_3, d_4, d_5, d_6, r_1, r_2, b_1, and b_3 are numeric (floating point) values.

Table 6. HF optimization of symmetry constrained $3\,C_{28}(3\times)$ cyclic polyyne cluster.

Variable	Initial values	Optimized values				
Basis set	STO-3G	STO-6G	3-21G	STO-3G	STO-6G	3-21G
a_1 (°)	62.3	66.79	67.5572	66.79	67.5572	68.8227
a_2 (°)	32.6	31.525	30.7715	31.525	30.7715	31.103
a_3 (°)	93.9	99.8835	100.7864	99.8835	100.7864	101.8435
a_4 (°)	73.4	67.8085	66.3221	67.8085	66.3221	73.1824
d_1 (°)	9.2	20.8758	21.8711	20.8758	21.8711	18.7214
d_2 (°)	264.5	288.0992	293.8228	288.0992	293.8228	304.1934
d_3 (°)	336	352.3978	352.396	352.3978	352.396	350.0585
d_4 (°)	101.7	79.8583	80.3866	79.8583	80.3866	86.638
d_5 (°)	252.1	259.5932	264.1909	259.5932	264.1909	282.1058
d_6 (°)	9.2	41.8704	44.3725	41.8704	44.3725	45.0033
r_1 (Å)	5.9	6.6069	6.8445	6.6069	6.8445	7.3985
r_2 (Å)	4.9	4.5177	4.6059	4.5177	4.6059	4.5938
b_1 (Å)	1.3586	1.3974	1.397	1.3974	1.397	1.3616
b_3 (Å)	1.2188	1.1866	1.1849	1.1866	1.1849	1.1969

Note: In each subsequent basis set, the initial values for the *ab-initio* optimization are taken from the optimized values of the previous basis set.

Table 7. BP optimization of symmetry constrained $3C_{28}(3\times)$ cyclic polyyne cluster.

Variable	Initial values	Optimized values				
Basis set	STO-3G	STO-6G	3-21G	STO-3G	STO-6G	3-21G
a_1 (°)	62.3	65.1494	65.0223	65.1494	65.0223	65.7197
a_2 (°)	32.6	43.8036	44.0403	43.8036	44.0403	45.0451
a_3 (°)	93.9	99.3011	98.9842	99.3011	98.9842	98.1413
a_4 (°)	73.4	66.8137	66.5817	66.8137	66.5817	65.6638
d_1 (°)	9.2	12.9403	13.0418	12.9403	13.0418	13.9321
d_2 (°)	264.5	273.2732	273.1815	273.2732	273.1815	274.306
d_3 (°)	336	350.7954	350.9283	350.7954	350.9283	356.6947
d_4 (°)	101.7	72.9921	72.3379	72.9921	72.3379	71.3572
d_5 (°)	252.1	254.6475	254.4274	254.6475	254.4274	252.8502
d_6 (°)	9.2	21.0582	20.4029	21.0582	20.4029	20.8467
r_1 (Å)	5.9	5.9349	5.9037	5.9349	5.9037	5.8302
r_2 (Å)	4.9	4.3368	4.3552	4.3368	4.3552	4.1621
b_1 (Å)	1.3586	1.3535	1.3533	1.3535	1.3533	1.326
b_3 (Å)	1.2188	1.2637	1.2637	1.2637	1.2637	1.2555

Note: In each subsequent basis set, the initial values for the DFT optimization are taken from the optimized values of the previous basis set.

unrefined , and this represents, on one hand, a limitation of the study, and offers the possibility of its further research on the other hand. Since the level of theory used in this study is limited to ab-intio HF and DFT BP, it is an ongoing project to submit the cluster for Møller Plesset methods (MP2 to MP4).

The study conducted on the systematic symmetry constrained optimization provides useful information. Data

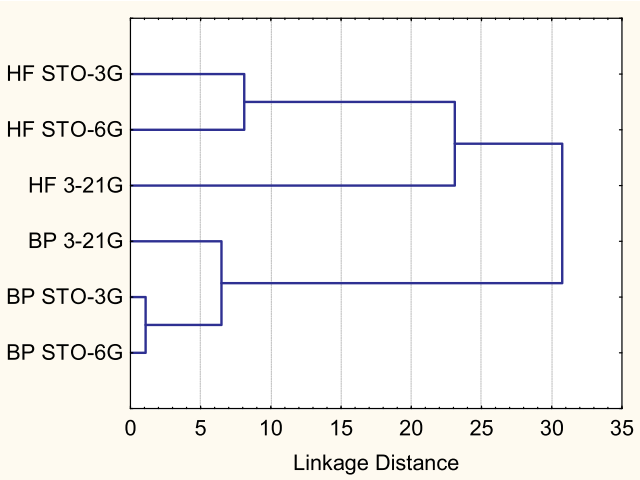

Figure 9. Clustering of classical ab-initio and DFT methods by euclidean distances of the symmetry constrained $3C_{28}(3\times)$ optimized values (data from Tables 6 and 7).

from Tables 6 and 7 has been used to obtain the Figure 9 plot.

Figure 9 shows that, both in the case of the HF method and in the case of the BP method, the increase in the number of basis functions (from 3 Gaussians to 6 Gaussians) does not produce significant changes in the values of the optimized parameters (therefore of the cluster location), while the polarization (3-21G in Figure 9) in both cases (HF and BP) brings a significant change. It is then expected that further increasing of the basis set (to cc-pVDZ[89]) shall produce new information.

However, the solution proposed by BP 3-21G and HF 3-21G differs the most of all (see the grouping in Figure 9) even if, as mentioned above, the values are very similar (the correlation between their values is 0.995).

3 $C_{28}(3\times)$ cluster is expected to have a good stability. Due to the presence of a large number of unsaturated bonds, it can be a precursor for hard materials. It is an interesting case [3] catenane. Since the rings are not actually connected, they are also expected to have great flexibility. Tuning a variety of properties and functionalization makes materials to be attractive for special applications, especially the ones from medicine and pharmacy.[90] Other applications include the ones covered in Refs. [91–93].

4. Conclusions

Bending of polyynes is a difficult task, and crossing rings of polyynes is even more challenging; modeling of the $_3C_{28}$ triple crossed C_{28} cyclic polyyne cluster proved it. However, the total energy of $3\,C_{28}(3\times)$ differs from the total energy of a system of 3 isolated C_{28} by about 0.01 Hartree, suggesting that $3\,C_{28}(3\times)$ is a stable configuration as well. The angles between the planes of the molecular rings (60.5°, 58.2°, and 61.7°) reveal almost an axial alignment of the rings (best visible at electronic densities in Figure 7) very close to a C_3 symmetry. The symmetry constrained optimization studies conducted using Z-matrix internal coordinates with Gaussian software have shown that the geometrical conformation of C_{28} polyyne as triple crossed cluster is a stable conformation, since in all scenarios the convergence is to nearby optimum local points, but only with small basis sets. Further studies with larger basis sets and upper theory level are required to validate these findings.

Acknowledgments

Help from the reviewers in improving the work was highly appreciated. This contribution was submitted and presented in behalf of NANOMOD (2023): NANO-SCI(ENCE) & NANO-TECH(NOLOGY) MANAGEMENT IN THE DIGITAL AND ARTIFICIAL INTELLIGENT ERA, Research International Workshop – Third Edition, Hosted by SIM 2023: REINVENTING MANAGEMENT IN TURBULENT TIMES, 20–21 October 2023, Timisoara, Romania.

Author contributions

C.E.S.: formal analysis, investigation, resources, validation, writing—review and editing; M.V.P.: writing—original draft preparation; L.J.: conceptualization, drawings, methodology, supervision.

Disclosure statement

No potential conflict of interest was reported by the authors.

Funding

This research received no external funding.

Data availability statement

Appendix A.3 contains atoms coordinates for $3C_{28}(3\times)$ cluster. Appendices A.4 and A.5 contain optimization output from symmetry constrained optimization of $3C_{28}(3\times)$ cluster (Appendix A.4 for *ab initio* and Appendix A.5 for *DFT*).

References

[1] Jones, E. R. H. Polyacetylenes. *Proc. Chem. Soc.* **1960**, 199–210. DOI: 10.1039/ps9600000193.
[2] Bohlmann, F.; Englisch, A.; Ottawa, N.; Sander, H.; Weise, W. Synthese des Cytisins. *Angew. Chem.* **1955**, *67*, 708–708. DOI: 10.1002/ange.19550672214.
[3] Sörensen, N. A. Some Naturally Occurring Acetylenic Compounds. *Proc. Chem. Soc.* **1961**, 98–110. DOI: 10.1039/PS9610000093.
[4] Bohlmann, F.; Bornowski, H.; Arndt, C. Die Chemie Von Triazin. *Fortschr. Chem. Forsch.* **1962**, *4*, 138–272.
[5] D, B. J. Polyacetylenes and Related Compounds in Nature. *Prog. Org. Chem.* **1964**, *6*, 86–134.
[6] Bohlmann, F. Natürlich Vorkommende Acetylen-Verbindungen. *Fortschr. Chem. Forsch* **1966**, *6*, 65–100.
[7] Kai, K.; Sogame, M.; Sakurai, F.; Nasu, N.; Fujita, M.; Collimonins, A. –D. Unstable Polyynes with Antifungal or Pigmentation Activities from the Fungus-Feeding Bacterium *Collimonas fungivorans* Ter331. *Org. Lett.* **2018**, *20*, 3536–3540. DOI: 10.1021/acs.orglett.8b01311.
[8] López, S.; Fernández-Trillo, F.; Midón, P.; Castedo, L.; Saá, C. Synthesis of Marine Polyacetylenes Callyberynes a–C by Transition-Metal-Catalyzed Cross-Coupling Reactions to sp Centers. *J. Org. Chem.* **2006**, *71*, 2802–2810. DOI: 10.1021/jo052609u.

[9] Listunov, D.; Maraval, V.; Chauvin, R.; Génisson, Y. Chiral Alkynylcarbinols from Marine Sponges: Asymmetric Synthesis and Biological Relevance. *Nat. Prod. Rep.* **2015**, *32*, 49–75. DOI: 10.1039/C4NP00043A.

[10] Zeni, G.; Panatieri, R. B.; Lissner, E.; Menezes, P. H.; Braga, A. L.; Stefani, H. A. Synthesis of Polyacetylenic Acids Isolated from *Heisteria acuminata*. *Org. Lett.* **2001**, *3*, 819–821. DOI: 10.1021/ol006946v.

[11] Kobaisy, M.; Abramowski, Z.; Lermer, L.; Saxena, G.; Hancock, R. E. W.; Towers, G. H. N., Doxsee, D.; Stokes, R. W. Antimycobacterial Polyynes of Devil's Club (*Oplopanax horridus*), a North American Native Medicinal Plant. *J. Nat. Prod.* **1997**, *60*, 1210–1213. DOI: 10.1021/np970182j.

[12] Meng, L.-Z.; Huang, W.-H.; Shao, L.; Wang, C.-Z.; Yuan, C.-S.; Zhou, H.-H. Anticancer Activities of Polyynes from the Root Bark of Oplopanax Horridus and Their Acetylated Derivatives. *Molecules* **2014**, *19*, 6142–6162. DOI: 10.3390/molecules19056142.

[13] Yamaguchi, M.; Park, H. J.; Ishizuka, S.; Omata, K.; Hirama, M. Chemistry and Antimicrobial Activity of Caryoynencin Analogs. *J. Med. Chem.* **1995**, *38*, 5015–5022. DOI: 10.1021/jm00026a008.

[14] Tada, M.; Chiba, K. Novel Plant Growth Inhibitors and an Insect Antifeedant from Chrysanthemum Coronarium (Japanese Name: Shungiku). *Agric. Biol. Chem.* **1984**, *48*, 1367–1369. DOI: 10.1080/00021369.1984.10866324.

[15] Lee, J.; Shi, Y. M.; Grün, P.; Gube, M.; Feldbrügge, M.; Bode, H.; Hennicke, F. Identification of Feldin, an Antifungal Polyyne from the Beefsteak Fungus *Fistulina hepatica*. *Biomolecules* **2020**, *10*, 1502. DOI: 10.3390/biom10111502.

[16] Fort, D. M.; King, S. R.; Carlson, T. J.; Nelson, S. T. Minquartynoic Acid from Coula Edulis. *Biochem. Syst. Ecol.* **2000**, *28*, 489–490. DOI: 10.1016/S0305-1978(99)00079-4.

[17] Rashid, M. A.; Gustafson, K. R.; Cardellina, J. H.; Boyd, M. R. Absolute Stereochemistry and anti-HIV Activity of Minquartynoic Acid, a Polyacetylene from *Ochanostachys amentacea* 1a. *Nat. Prod. Lett.* **2001**, *15*, 21–26. DOI: 10.1080/10575630108041253.

[18] Nakamura, Y.; Kawamoto, N.; Ohto, Y.; Torikai, K.; Murakami, A.; Ohigashi, H. A Diacetylenic Spiroketal Enol Ether Epoxide, AL-1, from *Artemisia lactiflora* Inhibits 12-O-Tetradecanoylphorbol-13-Acetate-Induced Tumor Promotion Possibly by Suppression of Oxidative Stress. *Cancer Lett.* **1999**, *140*, 37–45. DOI: 10.1016/S0304-3835(99)00048-8.

[19] Dang, Q. L.; Lim, C. H.; Kim, J. C. Current Status of Botanical Pesticides for Crop Protection. *Res. Plant Dis.* **2012**, *18*, 175–185. DOI: 10.5423/RPD.2012.18.3.175.

[20] Ardalan, T.; Ardalan, P.; Monajjemi, M. Nano Theoretical Study of a C16 Cluster as a Novel Material for Vitamin C Carrier. *Fuller. Nanotub. Carbon Nanostruct.* **2014**, *22*, 687–708. DOI: 10.1080/1536383X.2012.717561.

[21] Chianese, G.; Sirignano, C.; Shokoohinia, Y.; Mohammadi, Z.; Bazvandi, L.; Jafari, F.; Jalilian, F.; Schiano Moriello, A.; De Petrocellis, L.; Taglialatela-Scafati, O.; Rigano, D. TRPA1 Modulating C14 Polyacetylenes from the Iranian Endemic Plant *Echinophora platyloba*. *Molecules* **2018**, *23*, 23–1750. DOI: 10.3390/molecules23071750.

[22] Murata, K.; Suenaga, M.; Kai, K. Genome Mining Discovery of Protegenins a–D, Bacterial Polyynes Involved in the Antioomycete and Biocontrol Activities of Pseudomonas protegens. *ACS Chem. Biol.* **2022**, *17*, 3313–3320. DOI: 10.1021/acschembio.1c00276.

[23] Zheng, P.; Zubatyuk, R.; Wu, W.; Isayev, O.; Dral, P. O. Artificial Intelligence–Enhanced Quantum Chemical Method with Broad Applicability. *Nat. Commun.* **2021**, *12*, 7022. DOI: 10.1038/s41467-021-27340-2.

[24] Pan, B. T.; Xiao, J.; Li, J. L.; Liu, P.; Wang, C. X.; Yang, G. W. Carbyne with Finite Length: The One-Dimensional sp Carbon. *Sci. Adv.* **2015**, *1*, e1500857. DOI: 10.1126/sciadv.1500857.

[25] McCarthy, M. C.; Chen, W.; Travers, M. J.; Thaddeus, P. Microwave Spectra of 11 Polyyne Carbon Chains. *Astrophys. J. Suppl. S* **2000**, *129*, 611–623. DOI: 10.1086/313428.

[26] Jäntschi, L. *General Chemistry Course (Version 8)*; AcademicDirect: Cluj-Napoca, **2017**.

[27] Dubrovinskaia, N.; Dubrovinsky, L.; Crichton, W.; Langenhorst, F.; Richter, A. Aggregated Diamond Nanorods, the Densest and Least Compressible Form of Carbon. *Appl. Phys. Lett* **2005**, *87*, 83106. DOI: 10.1063/1.2034101.

[28] Itzhaki, L.; Altus, E.; Basch, H.; Hoz, S. Harder than Diamond: Determining the Cross-Sectional Area and Young's Modulus of Molecular Rods. *Angew. Chem. Int. Ed Engl.* **2005**, *44*, 7432–7435. DOI: 10.1002/anie.200502448.

[29] Monajjemi, M.; Lee, V. S.; Khaleghian, M.; Honarparvar, B.; Mollaamin, F. Theoretical Description of Electromagnetic Nonbonded Interactions of Radical, Cationic, and Anionic $NH_2BHNBHNH_2$ inside of the $B_{18}N_{18}$ Nanoring. *J. Phys. Chem. C* **2010**, *114*, 15315–15330. DOI: 10.1021/jp104274z.

[30] Monajjemi, M.; Boggs, J. E. A New Generation of B^nN^n Rings as a Supplement to Boron Nitride Tubes and Cages. *J. Phys. Chem. A* **2013**, *117*, 1670–1684. DOI: 10.1021/jp312073q.

[31] Jäntschi, L. Energetics of C8B8N8, N12B12, and C24 Macrocycles and Two [4]Catenanes. *Foundations* **2022**, *2*, 781–797. DOI: 10.3390/foundations2030053.

[32] Hirao, Y.; Daifuku, Y.; Ihara, K.; Kubo, T. Spin–Spin Interactions in One-Dimensional Assemblies of a Cumulene-Based Singlet Biradical. *Angew. Chem. Int. Ed Engl.* **2021**, *60*, 21319–21326. DOI: 10.1002/anie.202105740.

[33] Pinter, P.; Munz, D. Controlling Möbius-Type Helicity and the Excited-State Properties of Cumulenes with Carbenes. *J. Phys. Chem. A* **2020**, *124*, 10100–10110. DOI: 10.1021/acs.jpca.0c07940.

[34] Hoshi, K.; Yasuda, M.; Nakamura, T.; Yoshida, Y.; Ueta, S.; Minagawa, K.; Kawamura, Y.; Imada, Y.; Yagishita, F. Unexpected Formation of Poly-Functionalized Fulvenes by the Reaction of a Tetraaryl[5]Cumulene with Iodine. *Org. Biomol. Chem.* **2021**, *19*, 7594–7597. DOI: 10.1039/D1OB01270C.

[35] Martín-Fuentes, C.; Urgel, J. I.; Edalatmanesh, S.; Rodríguez-Sánchez, E.; Santos, J.; Mutombo, P.; Biswas, K.; Lauwaet, K.; Gallego, J. M.; Miranda, R.; et al. Cumulene-like Bridged Indeno[1,2-b]Fluorene π-Conjugated Polymers Synthesized on Metal Surfaces. *Chem. Commun. (Camb)* **2021**, *57*, 7545–7548. DOI: 10.1039/D1CC02058G.

[36] de la Torre, B.; Matěj, A.; Sánchez-Grande, A.; Cirera, B.; Mallada, B.; Rodríguez-Sánchez, E.; Santos, J.; Mendieta-Moreno, J. I.; Edalatmanesh, S.; Lauwaet, K.; et al. Tailoring p-Conjugation and Vibrational Modes to Steer on-Surface Synthesis of Pentalene-Bridged Ladder Polymers. *Nat. Commun.* **2020**, *11*, 4567. DOI: 10.1038/s41467-020-18371-2.

[37] Karpfen, A. Ab Initio Studies on Polymers. I. The Linear Infinite Polyyne. *J. Phys. C: Solid State Phys.* **1979**, *12*, 3227–3237. DOI: 10.1088/0022-3719/12/16/011.

[38] Sladkov, A. M.; Kasatochkin, V. I.; Kudryavtsev, Y. P.; Korshak, V. V. Synthesis and Properties of Valuable Polymers of Carbon. *Russ. Chem. Bull.* **1968**, *17*, 2560–2565. DOI: 10.1007/BF00907774.

[39] Akagi, K.; Nishiguchi, M.; Shirakawa, H.; Furukawa, Y.; Harada, I. One-Dimensional Conjugated Carbyne – Synthesis and Properties. *Synth. Met.* **1987**, *17*, 557–562. DOI: 10.1016/0379-6779(87)90798-3.

[40] Johnson, B. F. G.; Kakkar, A. K.; Khan, M. S.; Lewis, J. Synthesis of Novel Rigid Rod Iron Metal Containing Polyyne Polymers. *J. Organomet. Chem.* **1991**, *409*, C12–C14. DOI: 10.1016/0022-328X(91)80028-I.

[41] Rice, M. J.; Bishop, A. R.; Campbell, D. K. Unusual Soliton Properties of the Infinite Polyyne Chain. *Phys. Rev. Lett.* **1983**, *51*, 2136–2139. DOI: 10.1103/PhysRevLett.51.2136.

[42] Rozental, E.; Altus, E.; Major, D. T.; Hoz, S. Shaping Polyyne Rods by Using an Electric Field. *ChemistryOpen* **2017**, *6*, 733–738. DOI: 10.1002/open.201700132.

[43] Jäntschi, L.; Bolboacă, S. D. Conformational Study of C_{24} Cyclic Polyyne Clusters. *Int. J. Quant. Chem.* **2018**, *118*, e25614. DOI: 10.1002/qua.25614.

[44] Heimann, R. B. Linear Finite Carbon Chains (Carbynes): Their Role during Dynamic Transformation of Graphite to Diamond, and Their Geometric and Electronic Structure. *Diam. Relat. Mater.* **1994**, *3*, 1151–1157. DOI: 10.1016/0925-9635(94)90161-9.

[45] Page, A. J.; Ding, F.; Irle, S.; Morokuma, K. Insights into Carbon Nanotube and Graphene Formation Mechanisms from Molecular Simulations: A Review. *Rep. Prog. Phys.* **2015**, *78*, 36501. DOI: 10.1088/0034-4885/78/3/036501.

[46] Anderson, H. L.; Patrick, C. W.; Scriven, L. M.; Woltering, S. L. A Short History of Cyclocarbons. *BCSJ* **2021**, *94*, 798–811. DOI: 10.1246/bcsj.20200345.

[47] Eastmond, R.; Johnson, T. R.; Walton, D. R. M. Silylation as a Protective Method for Terminal Alkynes in Oxidative Couplings: A General Synthesis of the Parent Polyynes $H(C{\equiv}C)nH$ (n = 4-10. *Tetrahedron* **1972**, *28*, 4601–4616. DOI: 10.1016/0040-4020(72)80041-3.

[48] Zheng, Q; Gladysz, J.; A Synthetic Breakthrough into an Unanticipated Stability Regime: Readily Isolable Complexes in Which C_{16}–C_{28} Polyynediyl Chains Span Two Platinum Atoms. *J. Am. Chem. Soc.* **2005**, *127*, 10508–10509. DOI: 10.1021/ja0534598.

[49] Lagow, R. J.; Kampa, J. J.; Wei, H. C.; Battle, S. L.; Genge, J. W.; Laude, D. A.; Harper, C. J.; Bau, R.; Stevens, R. C.; Haw, J. F.; Munson, E. Synthesis of Linear Acetylenic Carbon: The "sp" Carbon Allotrope. *Science* **1995**, *267*, 362–367. DOI: 10.1126/science.267.5196.362.

[50] Hunter, J.; Fye, J.; Jarrold, M. F. Annealing C^{+}_{60} : Synthesis of Fullerenes and Large Carbon Rings. *Science* **1993**, *260*, 784–786. DOI: 10.1126/science.260.5109.784.

[51] Peggiani, S.; Facibeni, A.; Marabotti, P.; Vidale, A.; Scotti, S.; Casari, C. S. A Single Liquid Chromatography Procedure to Concentrate, Separate and Collect Size-Selected Polyynes Produced by Pulsed Laser Ablation in Water. *Fuller. Nanotub. Carbon Nanostructures* **2023**, *31*, 224–230. DOI: 10.1080/1536383X.2022.2137498.

[52] Allen, A. D.; Tidwell, T. T. Ketenes and Other Cumulenes as Reactive Intermediates. *Chem. Rev.* **2013**, *113*, 7287–7342. DOI: 10.1021/cr3005263.

[53] Ozcelik, A.; Aranda, D.; Gil-Guerrero, S.; Pola-Otero, X. A.; Talavera, M.; Wang, L.; Behera, S. K.; Gierschner, J.; Peña-Gallego, Á.; Santoro, F.; et al. Distinct Helical Molecular Orbitals through Conformational Lock. *Chemistry* **2020**, *26*, 17342–17349. DOI: 10.1002/chem.202002561.

[54] Anderson, B. D. Cyclic Polyynes as Examples of the Quantum Mechanical Particle on a Ring. *J. Chem. Educ* **2012**, *89*, 724–727. DOI: 10.1021/ed200439u.

[55] Jäntschi, L.; Bolboacă, S. D.; Janežic, D. Cyclic Carbon Polyynes. *Carbon Mater. Chem. Phys.* **2016**, *9*, 423–436. DOI: 10.1007/978-3-319-31584-3_23.

[56] Brémond, E.; Pérez-Jiménez, A.; Adamo, C.; Sancho-García, J. Stability of the Polyynic Form of C_{18},C_{22},C_{26} ,and C_{30} Nanorings: A Challenge Tackled by Range-Separated Double-Hybrid Density Functionals. *Phys. Chem. Chem. Phys.* **2022**, *24*, 4515–4525. DOI: 10.1039/d1cp04996h.

[57] Slanina, Z.; Zhao, X.; [Obar]sawa, E.; Adamowicz, L. Cyclic and Linear Structures of C13: A Computational Study. *Fullerene Sci. Technol.* **2000**, *8*, 369–383. DOI: 10.1080/10641220009351419.

[58] Barquera-Lozada, J. E. How to Bend a Cumulene. *Chemistry* **2020**, *26*, 4633–4639. DOI: 10.1002/chem.202000025.

[59] Hoffmann, R. Extended Hückel Theory—v: Cumulenes, Polyenes, Polyacetylenes and C_n. *Tetrahedron* **1966**, *22*, 521–538. DOI: 10.1016/0040-4020(66)80020-0.

[60] Hutter, J.; Luethi, H. P.; Diederich, F. Structures and Vibrational Frequencies of the Carbon Molecules C_2–C_{18} Calculated by Density Functional Theory. *J. Am. Chem. Soc.* **1994**, *116*, 750–756. DOI: 10.1021/ja00081a041.

[61] Springborg, M.; Kavan, L. On the Stability of Polyyne. *Chem. Phys.* **1992**, *168*, 249–258. DOI: 10.1016/0301-0104(92)87159-7.

[62] Springborg, M.; Kavan, L. Can Linear Carbon Chains Be Synthesized? *Synth. Met.* **1993**, *57*, 4405–4410. DOI: 10.1016/0379-6779(93)90757-N.

[63] Li, P. DFT Studies on Configurations, Stabilities, and IR Spectra of Neutral Carbon Clusters. *JAMS* **2012**, *3*, 308–322. DOI: 10.4208/jams.091411.101311a.

[64] Hartree, D. R. The Wave Mechanics of an Atom with a Non-Coulomb Central Field. Part I. Theory and Methods. *Math. Proc. Camb. Phil. Soc.* **1928**, *24*, 89–110. DOI: 10.1017/S0305004100011919.

[65] Hartree, D. R. The Wave Mechanics of an Atom with a non-Coulomb Central Field. Part II. Some Results and Discussion. *Math. Proc. Camb. Phil. Soc.* **1928**, *24*, 111–132. DOI: 10.1017/S0305004100011920.

[66] Fock, V. Näherungsmethode Zur Lösung Des Quantenmechanischen Mehrkörperproblems. *Z. Phys.* **1930**, *61*, 126–148. DOI: 10.1007/BF01340294.

[67] Fock, V. Selfconsistent Field MIt Austausch für Natrium. *Z. Physik* **1930**, *62*, 795–805. DOI: 10.1007/BF01330439.

[68] Hohenberg, P.; Kohn, W. Inhomogeneous Electron Gas. *Phys. Rev.* **1964**, *136*, B864–B871. DOI: 10.1103/PhysRev.136.B864.

[69] Kohn, W.; Sham, L. J. Self-Consistent Equations Including Exchange and Correlation Effects. *Phys. Rev.* **1965**, *140*, A1133–A1138. DOI: 10.1103/PhysRev.140.A1133.

[70] Becke, A. D. Density-Functional Exchange-Energy Approximation with Correct Asymptotic Behavior. *Phys. Rev. A Gen. Phys.* **1988**, *38*, 3098–3100. DOI: 10.1103/PhysRevA.38.3098.

[71] Perdew, J. P. Density-Functional Approximation for the Correlation Energy of the Inhomogeneous Electron Gas. *Phys. Rev. B Condens. Matter.* **1986**, *33*, 8822–8824. DOI: 10.1103/PhysRevB.33.8822.

[72] Lee, C.; Yang, W.; Parr, R. G. Development of the Colle-Salvetti Correlation-Energy Formula into a Functional of the Electron Density. *Phys. Rev. B Condens. Matter* **1988**, *37*, 785–789. DOI: 10.1103/PhysRevB.37.785.

[73] Becke, A. D. Density-Functional Thermochemistry. III. The Role of Exact Exchange. *J. Chem. Phys.* **1993**, *98*, 5648–5652. DOI: 10.1063/1.464913.

[74] Stephens, P. J.; Devlin, F. J.; Ashvar, C. S.; Chabalowski, C. F.; Frisch, M. J. Theoretical Calculation of Vibrational Circular Dichroism Spectra. *Faraday Disc.* **1994**, *99*, 103–119. DOI: 10.1039/fd9949900103.

[75] NIST. Experimental Data for N2 (Nitrogen Diatomic). Computational Chemistry Comparison and Benchmark DataBase Release 22. Standard Reference Database *101*, **2022**. http://cccbdb.nist.gov/exp2x.asp?casno=7727379.

[76] Hehre, W. J. *A Guide to Molecular Mechanics and Quantum Chemical Calculations*; Wavefunction, Inc.: Irvine, CA, **2003**.

[77] Diudea, M. V.; Gutman, I.; Jäntschi, L. *Molecular Topology*; Nova Science Publishers: Huntington, N.Y., **2001**.

[78] Joiţa, D. M.; Jäntschi, L. Extending the Characteristic Polynomial for Characterization of C20 Fullerene Congeners. *Mathematics* **2017**, *5*, 84. DOI: 10.3390/math5040084.

[79] Mezey, P. G. Cluster Topology and Bounds for the Electronic Energy. *Surf. Sci.* **1985**, *156*, 597–604. DOI: 10.1016/0039-6028(85)90230-4.

[80] Perepichka, D.; Bryce, M. Molecules with Exceptionally Small HOMO–LUMO Gaps. *Angew. Chem. Int. Ed. Engl.* **2005**, *44*, 5370–5373. DOI: 10.1002/anie.200500413.

[81] Weinhold, F. Why Do Cumulene Ketones Kink? *J. Org. Chem.* **2017**, *82*, 12238–12245. DOI: 10.1021/acs.joc.7b02089.

[82] Li, J. P.; Meng, S. H.; Lu, H. T.; Tohyama, T. First-Principles Study on the Mechanics, Optical, and Phonon Properties of Carbon Chains. *Chinese Phys. B* **2018**, *27*, 117101. DOI: 10.1088/1674-1056/27/11/117101.

[83] C_{84} Isomers. http://nanotube.msu.edu/fullerene/fullerene.php?C=84. Accessed June 4, 2023.

[84] Raghavachari, K.; Binkley, J. S. Structure, Stability, and Fragmentation of Small Carbon Clusters. *J. Chem. Phys.* **1987**, *87*, 2191–2197. DOI: 10.1063/1.453145.
[85] Zhou, J. J.; Park, J.; Lu, I. T.; Maliyov, I.; Tong, X.; Bernardi, M. Perturbo: A Software Package for ab Initio Electron–Phonon Interactions, Charge Transport and Ultrafast Dynamics. *Comput. Phys. Commun.* **2021**, *264*, 107970. DOI: 10.1016/j.cpc.2021.107970.
[86] Marini, G.; Marchese, G.; Profeta, G.; Sjakste, J.; Macheda, F.; Vast, N.; Mauri, F.; Calandra, M. EPIq: An Open-source Software for the Calculation of Electron-phonon Interaction Related Properties, , [arXiv: Cond-mat.mtrl-sci/2306.15462], **2023**.
[87] Baker, J.; Kessi, A.; Delley, B. The Generation and Use of Delocalized Internal Coordinates in Geometry Optimization. *J. Chem. Phys.* **1996**, *105*, 192–212. DOI: 10.1063/1.471864.
[88] Frisch, M. J.; Trucks, G. W.; Schlegel, H. B.; Scuseria, G. E.; Robb, M. A.; Cheeseman, J. R.; Scalmani, G.; Barone, V.; Mennucci, B.; Petersson, G. A. *Gaussian 09w Revision D.01*. Gaussian Inc., Wallingford CT, **2013**.
[89] Dunning, T. H. J. Gaussian Basis Sets for Use in Correlated Molecular Calculations. I. The Atoms Boron through Neon and Hydrogen. *J. Chem. Phys.* **1989**, *90*, 1007–1023. DOI: 10.1063/1.456153.
[90] Maitz, M. Applications of Synthetic Polymers in Clinical Medicine. *Biosurf. Biotribol.* **2015**, *1*, 161–176. DOI: 10.1016/j.bsbt.2015.08.002.
[91] Cataldo, F. Polyynes Formation from Electric Arc in Liquid Argon in Presence of Methane. *Fuller. Nanotub. Carbon Nanostruct.* **2007**, *15*, 291–301. DOI: 10.1080/15363830701423690.
[92] Kuzmin, S.; Duley, W. W. Ab Initio Calculations of Some Electronic and Vibrational Properties of Molecules Based on Multi-Layered Stacks of Cyclic C6. *Fuller. Nanotub. Carbon Nanostruct.* **2012**, *20*, 730–736. DOI: 10.1080/1536383X.2011.572314.
[93] Cataldo, F.; Ori, O.; Putz, M. V. From Graphyne to Cata-Condensed (Acenographynes) and Peri-Condensed PAHs-Graphyne Derivatives. *Fuller. Nanotub. Carbon Nanostruct.* **2018**, *26*, 535–544. DOI: 10.1080/1536383X.2018.1456426.

A. Appendix

A.1. Abbreviations

DFT	Density functional theory
Å	ångström (or angstrom),1Å=10^{-10}m
eV	electrnvolt (or electron-volt or electron volt),1eV = 1.602176634 10^{-19} kg m^2 s^{-2}
Hartree	Hartree atomic units,1Hartree = 27.211386245988 eV
°	angle degrees, $1^{\circ} = \frac{\pi}{180}$ rad
HOMO	Highest occupied molecular orbital
LUMO	Lowest unoccupied molecular orbital
RAMAN	Spectroscopic method named after Indian physicist C. V. Raman
IR	Infrared
STO	Slater type orbital (basis set)
STO-G	(or GTO) Gaussian type orbital (basis set; STO-3G is implicit)
STO-*n* G	STO-G with *n*Gaussian primitive functions used to represent each Slater type orbital
HF	Hartree–Fock method (see Table 1)
BP	Becke–Perdew (BP86) method (see Table 1)
BLYP	Becke–Lee–Yang–Parr method (see Table 1)
B3LYP	Becke-3–Lee–Yang–Parr method (see Table 1)

A.2. Cartesian coordinates (in Å) of carbon atoms contained in C_{28} cyclic polyyne having DFT BP 6-311G* optimal geometry.

Molecule is planar, so only two Coordinates are given for simplicity.

Spartan (software, v.14) has been used for getting the optimal geometry. Spartan manual can be consulted.

−3.779433103	−4.343710375
−4.631142557	−3.424159706
−5.292669253	−2.275493266
−5.660491878	−1.077310991
−5.757281127	0.244671659
−5.567718465	1.483622890
−5.079987547	2.716151210
−4.370856022	3.749620297
−3.396630015	4.648470698
−2.309363985	5.272030334
−1.041697758	5.659675350
0.208355728	5.750858847
1.518865689	5.551242431
2.684879472	5.091495646
3.779433103	4.343710375
4.631142557	3.424159706
5.292669253	2.275493266
5.660491878	1.077310991
5.757281127	−0.244671659
5.567718465	−1.483622890
5.079987547	−2.716151210
4.370856022	−3.749620297
3.396630015	−4.648470698
2.309363985	−5.272030334
1.041697758	−5.659675350
−0.208355728	−5.750858847
−1.518865689	−5.551242431
−2.684879472	−5.091495646

A.3. Cartesian coordinates (in Å) of Carbon atoms contained in the triple crossed $3\,C_{28}$ cyclic polyyne having DFT BP 6-311 G* optimal geometry.

Spartan (software, v.14) has been used for getting the optimal geometry. Spartan manual can be consulted.

0.1081099	−2.1978698	3.8124512
1.2056420	−2.5713773	4.4555381
2.3745993	−2.8035879	4.8441297
3.6863887	−2.9116560	5.0033492
4.9358079	−2.8791816	4.9069525
6.2001238	−2.7066612	4.5470617
7.2807209	−2.4215462	3.9791452
8.2436938	−2.0052123	3.1684376
8.9398554	−1.5232311	2.2440214
9.4139513	−0.9437117	1.1498015
9.5900473	−0.3560606	0.0565915
9.4818781	0.2758469	−1.1039324
9.1042923	0.8544556	−2.1498199
8.4366822	1.4200845	−3.1459362
7.5785190	1.8828667	−3.9337875
6.4809132	2.2755954	−4.5652008
5.3131904	2.5363976	−4.9388127
4.0031279	2.6808997	−5.0827568
2.7549156	2.6839583	−4.9677454
1.4903046	2.5439170	−4.5953856
0.4105097	2.2777469	−4.0170021
−0.5524150	1.8656063	−3.2043640
−1.2444176	1.3681746	−2.2853310
−1.7137480	0.7556803	−1.2074914
−1.8873110	0.1254540	−0.1381240
−1.7816684	−0.5500088	0.9975765
−1.4101103	−1.1594220	2.0278757
−0.7462742	−1.7384596	3.0186326
−4.4606433	3.8686637	−0.1870985
−5.1464851	2.7343337	−0.1948037
−5.5451295	1.5460553	−0.1810954
−5.6882972	0.2287257	−0.1496552
−5.5577526	−1.0173385	−0.1084324
−5.1442587	−2.2758050	−0.0611870
−4.5083814	−3.3551146	−0.0165263
−3.5980836	−4.3179593	0.0252508
−2.5542884	−5.0113564	0.0586056
−1.3111197	−5.4712020	0.0877242
−0.0671116	−5.6239169	0.1109824
1.2499365	−5.4734415	0.1347020
2.4289644	−5.0484925	0.1574144
3.5403005	−4.3261955	0.1862500
4.4102730	−3.4241556	0.2141999
5.0963185	−2.2903338	0.2476081
5.4988420	−1.1035063	0.2751556
5.6455254	0.2138363	0.2955182
5.5173109	1.4607760	0.3022932
5.1015330	2.7194560	0.2929751
4.4614119	3.7969227	0.2662062
3.5472692	4.7560978	0.2213098
2.5023265	5.4461309	0.1632029
1.2599976	5.9038618	0.0934927
0.0179730	6.0576835	0.0223661
−1.2975432	5.9095744	−0.0507637
−2.4766433	5.4884201	−0.1105259
−3.5894027	4.7694705	−0.1599784
1.8648041	0.3702204	0.4728939
1.8727378	−0.2960981	−0.6729266
1.6101058	−0.9152399	−1.7305072
1.0470566	−1.5210852	−2.7665952
0.2743915	−2.0173245	−3.6196773
−0.7586990	−2.4366183	−4.3368480
−1.8868965	−2.7171376	−4.8056120
−3.1795975	−2.8774223	−5.0523258
−4.4328297	−2.8973257	−5.0399323
−5.7246598	−2.7775973	−4.7671401
−6.8540821	−2.5413744	−4.2773276
−7.8906754	−2.1707457	−3.5385499
−8.6746229	−1.7247151	−2.6679795
−9.2532276	−1.1705672	−1.6114549
−9.5350084	−0.5971144	−0.5329807
−9.5394582	0.0329792	0.6335454
−9.2641033	0.6220048	1.7053265
−8.6923268	1.2069386	2.7489075
−7.9127070	1.6970728	3.5994907
−6.8796315	2.1262970	4.3109862
−5.7527731	2.4280803	4.7700155
−4.4629543	2.6220539	5.0078198
−3.2106523	2.6755248	4.9844929
−1.9183921	2.5886917	4.7013097
−0.7891786	2.3717444	4.2016114
0.2458454	2.0093422	3.4567272
1.0225097	1.5539361	2.5846084
1.5903183	0.9769541	1.5348453

(*continued*)

A.4. Gaussian HF 3-21G optimization output

1|1|UNPC-LORI1-D61F37D5A|POpt|RHF|3-21G|C84|LORI1|24-Jun-2022|1||#P rhf/3-21g int = ultrafine opt=(Z-matrix,maxcycle = 1000)||3C28 polyyne optimization||0,1|C|C,1,b1|C,2,b3,1,a0|C,3,b1,2,a0,1,d0,0|C,4,b3,3,a0,2,d0,0|C,5,b1,4,a0,3,d0,0|C,6,b3,5,a0,4,d0,0|C,7,b1,6,-a0,5,d0,0|C,8,b3,7,a0,6,d0,0|C,9,b1,8,a0,7,d0,0|C,10,b3,9,a0,8,d0,0|C,11,-b1,10,a0,9,d0, 0|C,12,b3,11,a0,10,d0,0|C,13,b1,12,a0,11,d0,0|C,14, b3,13, a0,12,d0,0|C,15,b1,14,a0,13,d0,0|C,16,b3,15,a0,14,d0,0|C,17,b1,16,a0,15,-d0,0|C,18,b3,17,a0,16,d0,0|C,19,b1,18,a0,17,d0,0|C,20,b3,19,a0,18,d0, 0|C,21,b1,20,a0,19,d0,0|C,22,b3,21,a0,20,d0,0|C,23,b1,22,a0,21,d0,0|C,24,-b3,23,a0,22,d0, 0|C,25,b1,24,a0,23,d0,0|C,26,b3,25,a0,24,d0,0|C,27,b1,26, a0,25,d0,0|C,28,r1,27,a1,26,d1,0|C,29,b1,28,a2,27,d2,0|C,30,b3,29,a0,28, d5,0|C,31,b1,30,a0,29,d0,0|C,32,b3,31,a0,30,d0,0|C,33,b1,32,a0,31,d0,0| C,34,b3,33,a0,32,d0,0|C,35,b1,34,a0,33,d0,0|C,36,b3,35,a0,34,d0,0|C,37, b1,36,a0,35,d0,0|C,38,b3,37,a0,36,d0,0|C,39,b1,38,a0,37,d0,0|C,40,b3,39, a0,38,d0,0|C,41,b1,40,a0,39,d0,0|C,42,b3,41,a0,40,d0,0|C,43,b1,42,a0,41, d0,0|C,44,b3,43,a0,42,d0,0|C,45,b1,44,a0,43,d0,0|C,46,b3,45,a0,44,d0,0| C,47,b1,46,a0,45,d0,0|C,48,b3,47,a0,46,d0,0|C,49,b1,48,a0,47,d0,0|C,50, b3,49,a0,48,d0,0|C,51,b1,50,a0,49,d0,0|C,52,b3,51,a0,50,d0,0|C,53,b1,52, a0,51,d0,0|C,54,b3,53,a0,52,d0,0|C,55,b1,54,a0,53,d0,0|C,56,r2,55,a3,54, d3,0|C,57,b1,56,a4,55,d4,0|C,58,b3,57,a0,29,d6,0|C,59,b1,58,a0,57, d0,0|C,60,b3,59,a0,58,d0,0|C,61,b1,60,a0,59,d0,0|C,62,b3,61,a0,60,d0,0| C,63,b1,62,a0,61,d0,0|C,64,b3,63,a0,62,d0,0|C,65,b1,64,a0,63,d0,0|C,66, b3,65,a0,64,d0,0|C,67,b1,66,a0,65,d0,0|C,68,b3,67,a0,66,d0,0|C,69,b1,68, a0,67,d0,0|C,70,b3,69,a0,68,d0,0|C,71,b1,70,a0,69,d0,0|C,72,b3,71,a 0,70,d0,0|C,73,b1,72,a0,71,d0,0|C,74,b3,73,a0,72,d0,0|C,75,b1,74,a0,73, d0,0|C,76,b3,75,a0,74,d0,0|C,77,b1,76,a0,75,d0,0|C,78,b3,77,a0,76,d0, 0|C,79,b1,78,a0,77,d0,0|C,80,b3,79,a0,78,d0,0|C,81,b1,80,a0,79,d0,0|C, 82,b3,81,a0,80,d0,0|C,83,b1,82,a0,81,d0,0||a1 = 68.82269519|a2 = -31.10297214|a3 = 101.84348727|a4 = 73.18241043|d1 = 18.721 39501| d2 = 304.19338238|d3 = 350.05847216|d4 = 86.63802695|d5 = 282.10579 528|d6 = 45.00331832|r1 = 7.39854905|r2 = 4.59380302|b1 = 1.36155233| b3 = 1.1969261 |a0 = 167.14|d0 = 0.||Version = IA32W-G09RevD. 01| State = 1-A|HF=-3160.7111467|RMSD = 6.693e-009|RMSF = 2.698e-003|Dipole=-0.002818,0.0012891,-0.0008313|Quadrupole = 0.0197528,-2.5311908,2.511438,0.0189819,0.5778629,-0.040869|PG = C01 [X(C84)]||@

A.5. Gaussian BP 3-21 G optimization output

1|1|UNPC-LORI2-168025F00|POpt|RBP86|3-21G|C84|LORI2|21-Jun-2022|1||#Pbp86/3-21g opt=(Z-matrix,maxcycle = 1000)||3C28 polyyne optimization||0,1|C|C,1,b1|C,2,b3,1,a0|C,3,b1,2,a0,1,d0,0|C,4,b3, 3, a0,2,d0,0|C,5,b1,4,a0,3,d0,0|C,6,b3,5,a0,4,d0,0|C,7,b1,6,a0,5,d0,0|C,8,-b3,7,a0,6,d0,0|C,9,b1,8,a0,7,d0,0|C,10,b3,9,a0,8,d0,0|C,11,b1,10,a0,9,d0, 0|C,12,b3,11,a0,10,d0,0|C,13,b1,12,a0,11,d0,0|C,14,b3,13,a0,12,d0,0|C,15, b1,14,a0,13,d0,0|C,16,b3,15,a0,14,d0,0|C,17,b1,16,a0,15,d0,0|C,18,b3,17, a0,16,d0,0|C,19,b1,18,a0,17,d0,0|C,20,b3,19,a0,18,d0,0|C,21,b1,20,a0,19, d0,0|C,22,b3,21,a0,20,d0,0|C,23,b1,22,a0,21,d0,0|C,24,b3,23,a0,22,d0,0| C,25,b1,24,a0,23,d0,0|C,26,b3,25,a0,24,d0,0|C,27,b1,26,a0,25,d0,0|C,28,-r1,27,a1,26,d1,0|C,29,b1,28,a2,27,d2,0|C,30,b3,29,a0,28,d5,0|C,31,b1,30, a0,29,d0,0|C,32,b3,31,a0,30,d0,0|C,33,b1,32,a0,31,d0,0|C,34,b3,33,a0,32, d0,0|C,35,b1,34,a0,33,d0,0|C,36,b3,35,a0,34,d0,0|C,37,b1,36,a0,35,d0,0| C,38,b3,37,a0,36,d0,0|C,39,b1,38,a0,37,d0,0|C,40,b3,39,a0,38,d0,0|C,41,

b1,40,a0,39,d0,0|C,42,b3,41,a0,40,d0,0|C,43,b1,42,a0,41,d0,0|C,44,b3,43,a0,42,d0,0|C,45,b1,44,a0,43,d0,0|C,46,b3,45,a0,44,d0,0|C,47,b1,46,a0,45,d0,0|C,48,b3,47,a0,46,d0,0|C,49,b1,48,a0,47,d0,0|C,50,b3,49,a0,48,d0,0|C,51,b1,50,a0,49,d0,0|C,52,b3,51,a0,50,d0,0|C,53,b1,52,a0,51,d0,0|C,54,b3,53,a0,52,d0,0|C,55,b1,54,a0,53,d0,0|C,56,r2,55,a3,54,d3,0|C,57,b1,56,a4,55,d4,0|C,58,b3,57,a0,29,d6,0|C,59,b1,58,a0,57,d0,0|C,60,b3,59,a0,58,d0,0|C,61,b1,60,a0,59,d0,0|C,62,b3,61,a0,60,d0,0|C,63,b1,62,a0,61,d0,0|C,64,b3,63,a0,62,d0,0|C,65,b1,64,a0,63,d0,0|C,66,b3,65,a0,64,d0,0|C,67,b1,66,a0,65,d0,0|C,68,b3,67,a0,66,d0,0|C,69,b1,68,a0,67,d0,0|C,70,b3,69,a0,68,d0,0|C,71,b1,70,a0,69,d0,0|C,72,b3,71,a0,70,d0,0|C,73,b1,72,a0,71,d0,0|C,74,b3,73,a0,72,d0,0|C,75,b1,74,a0,73,d0,0|C,76,b3,75,a0,74,d0,0|C,77,b1,76,a0,75,d0,0|C,78,b3,77,a0,76,d0,0|C,79,b1,78,a0,77,d0,0|C,80,b3,79,a0,78,d0,0|C,81,b1,80,a0,79,d0,0|C,82,b3,81,a0,80,d0,0|C,83,b1,82,a0,81,d0,0||a1 = 65.71968059|a2 = 45.04512007|a3 = 98.1413297|a4 = 65.66384224|d1 = 13.93209615|d2 = 274.30604399|d3 = 356.69473231|d4=71.35717573|d5 = 252.85024743|d6 = 20.84669559|r1 = 5.83023522|r2 = 4.1621058 5|b1= 1.32601129|b3 = 1.25554015|a0 = 167.14|d0 = 0.||Version = IA32W-G09RevD.01|State = 1-A|HF=-3180.9495537|RMSD = 5.289e-009|RMSF = 1.780e-003|Dipole=-0.0051594,0.0004384,-0.002094|Quadrupole=-0.3168178,-1.1323997,1.4492175,0.0081239,0.7021836,-0.0101094|PG = C01 [X(C84)]||@